TOFIELD, B. C. (1982). *Intercalation Chemistry*, edited by A. J. JACOBSON & M. S. WHITTINGHAM, pp. 181–227. New York: Academic Press.

WALKER, J. R. & CATLOW, C. R. A. (1982). *J. Phys. C*, **15**, 6151–6161.

WANG, J. C. (1980). *J. Chem. Phys.* **73**, 5786–5795.

WHITTINGHAM, M. S. & HUGGINS, R. A. (1971). *J. Electrochem. Soc.* **118**, 1–6.

WOLF, D. (1979). *J. Phys. Chem. Solids*, **40**, 757–773.

YAO, Y. F. & KUMMER, J. T. (1967). *J. Inorg. Nucl. Chem.* **29**, 2453–2474.

ZENDEJAS, M. A. & THOMAS, J. O. (1990). *Phys. Scr.* In the press.

A Single-Crystal X-ray Diffraction Study of the Ion Exchange of Cd^{2+} into Ag^+ β-Alumina

By KRISTINA EDSTRÖM AND JOHN O. THOMAS

Institute of Chemistry, University of Uppsala, Box 531, S-751 21 Uppsala, Sweden

AND GREGORY C. FARRINGTON

Department of Materials Science and Engineering K1, University of Pennsylvania, Philadelphia, PA 19104, USA

Abstract

Conventional single-crystal X-ray diffraction (Mo $K\alpha$ radiation, $\lambda = 0.71073$ Å) at 295 K has been used to study the ionic distribution of five compositions of the mixed-cation system Ag^+/Cd^{2+} β-alumina, $Ag_{1.22-y}Cd_{y/2}Al_{11}O_{17.11}$, $y = 0.00$, 0.10, 0.41, 0.99 and 1.11. $M_r = 702.1$, 697.1, 680.7, 651.1 and 644.8, $F(000) = 674.4$, 670.0, 655.4, 629.0 and 623.4. The compounds are made by the controlled ion exchange of Cd^{2+} ions into Ag^+ β-alumina from a $CdCl_2$ melt at 873 K. The structure comprises a hexagonal framework of spinel-type blocks of aluminium oxide separating two-dimensional conduction planes with a spacing of ~ 11 Å. All atoms in the spinel framework follow the centrosymmetric hexagonal space group $P6_3/mmc$, $Z = 2$, with cell dimensions $a = 5.5914$ (3), 5.6032 (2), 5.5959 (2), 5.5896 (5) and 5.5900 (7) Å and $c = 22.430$ (4), 22.504 (3), 22.458 (1), 22.434 (8) and 22.396 (6) Å for $y = 0.00$, 0.10, 0.41, 0.99 and 1.11, respectively. Final $wR(F_o^2)$ values are 0.0796, 0.0693, 0.0698, 0.0874 and 0.0853, respectively. In Ag^+ β-alumina, the Ag^+ ions occupy three different $6(h)$ sites: one near the $2(d)$ site, Ag(1); one close to the $2(b)$ site, Ag(3); and a third site, Ag(2), between these two sites, close to Ag(1). The occupations are 41, 33 and 26% for Ag(1), Ag(2) and Ag(3), respectively. The Cd^{2+} ions enter a new $6(h)$ site, not previously occupied by Ag^+ ions. At low replacement (~ 8%), the Ag(1)-site occupation is unchanged. By the time ~ 34% of the Ag^+ ions have been replaced, three Ag^+ sites are replaced with almost equal amounts by Cd^{2+} ions. When 81 and 91% of the Ag^+ ions have been replaced, Ag(1) is the only site still containing Ag^+ ions. The implications of these results are discussed with reference to the general aspects of ion exchange in β-alumina.

Introduction

The Na^+ β-alumina structure offers a unique opportunity for studying the behaviour of mixed cations with different radii and valence because different monovalent cation types can be accommodated into the same structural host (Yao & Kummer, 1967). The structure comprises loosely packed conduction layers which interleave rigid spinel blocks. More recently, Na^+ β-alumina has been exploited as a host for probing the structural and chemical properties of mixed-cation systems, typically, the non-additive behaviour of ionic conductivity of mixed-alkali systems which is a phenomenon commonly referred to as the mixed alkali effect, *e.g.* Na^+–K^+ and Na^+–Ag^+ β-alumina (Bruce, Howie & Ingram, 1986) and Na^+–Li^+ β-alumina (Tofield & Farrington, 1979).

In contrast, divalent ions are found to be reluctant to exchange into β-alumina and the resulting compounds are poor ionic conductors (unlike the situation in the related compound β''-alumina, which accepts a diversity of divalent ions). It has been found that Cd^{2+} is the only divalent cation type which can exchange totally into β-alumina and that this process can serve as a valuable structural probe

of the Na^+-conductivity mechanism. Studies of the Na^+–Cd^{2+} β-alumina system (Sutter, Cratty, Saltzberg & Farrington, 1983; Catti, Cazzanelli, Ivaldi & Mariotto, 1987; Edström, Thomas & Farrington, 1988, 1991) have thus shown that the local structure of the Na^+ ions is critical to the Na^+-conduction mechanism. Since it is known that the distribution of Ag^+ ions in the conduction plane of β-alumina (Roth, 1972; Boilot, Colomban, Collongues, Collin & Comès, 1980) is qualitatively different from that of Na^+ ions in Na^+ β-alumina (Roth, Reidinger & LaPlaca, 1976; Reidinger, 1979; Edström et al., 1991) the suggestion arises that we can extend our understanding of conduction mechanisms in β-alumina by also following the effect of the systematic substitution of Cd^{2+} ions into the Ag^+ β-alumina system. The Cd^{2+} ions can be assumed to be trapped in the structure at temperatures below 700 K (Sutter et al., 1983) and the ionic mobility can be attributed solely to Ag^+ ions. This assumption will be reflected in the structural arrangement of ions in the conduction plane. This method is also a useful approach for resolving structural overlap found in an X-ray diffraction investigation.

It should finally be pointed out that several mechanisms are possible for the compensation of the excess positive charge in the conduction plane of β-alumina: a trivalent aluminium ion in the spinel block can be exchanged for a divalent ion; alternatively, a Roth–Reidinger defect can exist involving an extra oxygen ion in the conduction plane structurally supported by interstitial aluminium ions in the spinel block (Roth et al. 1976; Reidinger, 1979). A combination of both mechanisms can also occur. In this study, only structures with Roth–Reidinger-defect compensation are considered.

Furthermore, it should be noted that Ag^+ and Cd^{2+} ions possess the same number of electrons and cannot, therefore, be distinguished explicitly in an X-ray diffraction experiment.

Experimental

Crystal preparation

Ag^+ β-alumina was prepared from Na^+ β-alumina (obtained from Union Carbide Corporation) by ion exchange in $AgNO_3$ at 575 K. The degree of exchange was monitored by using ^{22}Na as a radiotracer. These crystals were then annealed overnight at 775 K. This procedure was repeated several times. The fully exchanged Ag^+ β-alumina crystals were then suspended in a $CdCl_2$ melt at 873 K for different periods of time. The degree of exchange was monitored by careful weight measurements (Table 1). The crystals were then annealed again at 923 K to

Table 1. *Composition of the five different crystals studied in the system* $Ag_{1.22\ y}Cd_{y/2}Al_{11}O_{17.11}$ *as obtained from different analysis techniques*

y	Formula derived from diffraction experiment ($O_{17.11}$ assumed)	Weight measurement	Linear absorption measurement	Microprobe analysis
0·00	$Ag_{1.22}Al_{11}O_{17.11}$		0·00 (2)	0·0 (1)
0·10	$Ag_{1.12}Cd_{0.05}Al_{11}O_{17.11}$	0·1 (1)	0·10 (2)	0·1 (1)
0·41	$Ag_{0.81}Cd_{0.20}Al_{11}O_{17.11}$	0·4 (1)	0·42 (2)	0·4 (1)
0·99	$Ag_{0.23}Cd_{0.49}Al_{11}O_{17.11}$	0·7 (1)	0·74 (2)	0·7 (1)
1·11	$Ag_{0.12}Cd_{0.55}Al_{11}O_{17.11}$	1·2 (1)	1·12 (2)	1·0 (1)

allow the Cd^{2+} ions to distribute evenly. Five appropriate compositions were selected for the X-ray diffraction study. As extra checks on composition, the ratio of Ag^+ to Cd^{2+} ions in the crystals was also measured by microprobe analysis, an X-ray linear absorption measurement and chemical analysis (Table 1). The average compositions from the analyses were assumed in the refinements.

Data collection

Experimental details are summarized in Table 2 and a few remarks may be added. The quality of each crystal used was checked with Laue films. Single-crystal intensities were measured at 295 K with a Stoe automatic four-circle diffractometer controlled by a MicroVAXII computer. Integrated intensities were measured using an $\omega/2\theta$ step scan (80 steps) and corrected for background (Lehmann & Larsen, 1974); the correction was modified to allow for the $K\alpha$ doublet according to Blessing, Coppens & Becker (1974). Five standard reflections were used in each case to scale intensities and standard deviations (McCandlish, Stout & Andrews, 1975). Lp and absorption corrections were applied, the latter using an explicit description of crystal size and shape. Cell parameters were determined from a least-squares fit to observed 2θ angles prior to data collection. Systematic absences indicated the possible space groups $P6_3/mmc$ and $P6_3mc$.

Refinements

Ag^+ β-alumina has been studied previously (Boilot, Colomban, Collin & Comès, 1980) (see Fig. 1). Parameters from this study (within space group $P6_3/mmc$) were used as starting parameters in the refinement of Ag^+ β-alumina (Figs. 2a and 2f). Different models describing the Ag^+ ion near BR (Beevers–Ross site) [Ag(1) at BRD1 site] were tested and a split-atom model was found to be the most appropriate. The same test was carried out for Ag(3) at the aBR (anti-Beevers–Ross) site and here also a split-atom model was better. Thermal vibrations and/or displacements were described with anisotropic β_{ij} tensors for all Ag^+ ions. The Roth–Reidinger defect was included with the extra O(6)

Table 2. *Some experimental parameters relating to the data collections and refinements for* $Ag_{1\cdot22-y}Cd_{y/2}$ $Al_{11}O_{17\cdot11}$, $y = 0\cdot00$, $0\cdot10$, $0\cdot41$, $0\cdot99$ *and* $1\cdot11$

	$y = 0\cdot00$	$y = 0\cdot10$	$y = 0\cdot41$	$y = 0\cdot99$	$y = 1\cdot11$
$F(000)$	674·4	669·8	655·6	629·0	623·4
Cell parameters (Å)					
a	5·5914 (3)	5·6032 (2)	5·5959 (1)	5·5896 (1)	5·5900 (7)
c	22·430 (4)	22·504 (3)	22·458 (1)	22·434 (8)	22·396 (6)
Cell volume (Å³)	607·29	611·88	609·03	607·01	606·07
No. of reflections for cell determination	25	24	24	24	24
2θ range ( )	14 30	14–30	14–30	25· 30	25·30
D_x (Mg m⁻¹)	3·84	3·78	3·71	3·56	3·53
Max./min. crystal dimensions (mm)	0·18/0·13	0·21/0·13	0·18/0·14	0·17/0·11	0·18/0·13
μ_x (mm⁻¹)	2·93	2·75	2·54	2·24	2·15
μ_c (mm⁻¹)	2·88	2·74	2·60	2·30	2·08
Transmission factors	0·61–0·70	0·66–0·73	0·71–0·77	0·73 0·80	0·64–0·87
$(\sin\theta/\lambda)_{max}$ (Å⁻¹)	1·07	1·08	1·08	1·08	1·08
hkl range h	−10 0	0 10	0 10	0–10	−10·0
k	−10–0	0–10	0–10	0–10	0–10
l	0–47	−48 0	−48–0	0–48	0–48
K factor in empirical weighting scheme	0·02	0·02	0·02	0·04	0·04
Max./min. peak in final difference map (e Å⁻³)	2·11/−1·39	2·21/−2·01	1·67/−1·15	0·91/−0·76	0·82/−1·51
No. of standard reflections	5	5	5	5	5
No. of observed reflections	2254	2454	2448	2061	4665
$R_{int} = \Sigma I_o - \bar{I}_o / \Sigma I_o$	0·036	0·034	0·034	0·047	0·049
No. of unique reflections	1245	1293	1289	1184	1387
No. of parameters refined	53	55	56	52	59
No. of reflections used in refinement $[F_o^2 > 2\sigma(F^2)]$	1634	1859	1828	1598	3301
$R(F_o)$	0·0368	0·0321	0·0349	0·0410	0·0381
$R(F_o^2)$	0·0567	0·0371	0·0459	0·0821	0·0765
$wR(F_o^2)$	0·0796	0·0693	0·0698	0·0874	0·0853
S	1·7837	1·7747	1·7018	1·6391	1·3850
Max. Δ/σ	0·1	0·1	0·1	0·1	0·1

atom fixed at a mid-oxygen (mO) site [midway between column-oxygens O(5)] in the conduction pathway and given an isotropic temperature factor. The interstitial Al(5) atoms were found above and below the conduction plane (at $z \sim 0\cdot175$ and $z \sim 0\cdot325$) and their positional parameters were refined. The Al(5) occupation was initially refined; the value obtained corresponded to that of the fixed O(6), *i.e.* 0·11 per cell layer. The thermal vibrational description for Al(5) was constrained to be the same as that for Al(1) and the occupation of Al(1) was reduced by an amount corresponding to the occupation of Al(5). Remarkably, the total Ag^+-ion content in the conduction plane refined without constraints to the expected value of 1·22. A cation charge of 1·22 was then assumed in the refinement of the mixed crystals.

In three mixed-ion structures, the Cd^{2+}-ion occupation was constrained to values obtained from the analyses and the Ag^+ content constrained to give a total cation charge in the conduction plane of 1·22. In the case of one composition, $y = 0\cdot99$, the different models tested in the refinements gave a result

with more Cd^{2+} ions in the structure than obtained from analysis.

An initial crude picture of the conduction plane in the $y = 0\cdot10$ case was obtained from a difference Fourier synthesis after the parameters for pure Ag^+ β-alumina were used to obtain the F_c's. The best fit was obtained by assigning the electron density in the difference maps to Cd^{2+} at a new 6(h) site (B site) (Figs. 2b and 2g and Table 3).* The occupation of the BRD1 site could be kept to the same value as in Ag^+ β-alumina. The Ag^+ occupations of the other two sites were coupled in the refinement. Anisotropic β_{ij}'s were used for the description of the thermal vibration/displacement.

A crude picture for the $y = 0\cdot41$ structure was obtained as for $y = 0\cdot10$. The same Cd^{2+} site was found and refined (Figs. 2c and 2h and Table 3). The Ag^+-ion occupations of BRD1 and BRD2 [Ag(1) and Ag(2)] were coupled and the occupation of the Ag(3) site near aBR was fixed empirically to a value consistent with a clean Fourier difference map.

For the $y = 0\cdot99$ crystal, Cd^{2+} ions were again found in the B site, the site near aBR was almost empty and the remaining Ag^+ was found in the BRD1 site (Figs. 2d and 2i). Anisotropic β_{ij}'s were again used for Ag^+ and Cd^{2+} ions. The Ag^+-ion occupation of the BRD1 site was coupled to the Cd^{2+} occupation of the B site. Some difficulties were experienced in these refinements as the total Cd^{2+} content could not be made consistent with the analysis results. We were forced to conclude that this was indeed a real effect and that the small single crystal for the data collection did not have the same composition as the larger crystal from which it was removed (see Table 1).

The $y = 1\cdot11$ crystal contained fewer Cd^{2+} ions than expected on the basis of weight measurements but the refined result was consistent with results from the other analyses. The measured c axis (22·40 Å) (Table 2) compared to that of Cd^{2+} β-alumina (22·37 Å) (Edström *et al.*, 1991) supports the determination of the $y = 1\cdot11$ composition. Also, the BR site is not empty, unlike the situation for Cd^{2+}
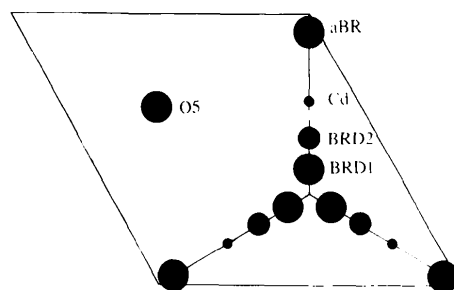
Fig. 1. A schematic representation of the different sites occupied by Ag⁺ and Cd²⁺ ions in the conduction plane.
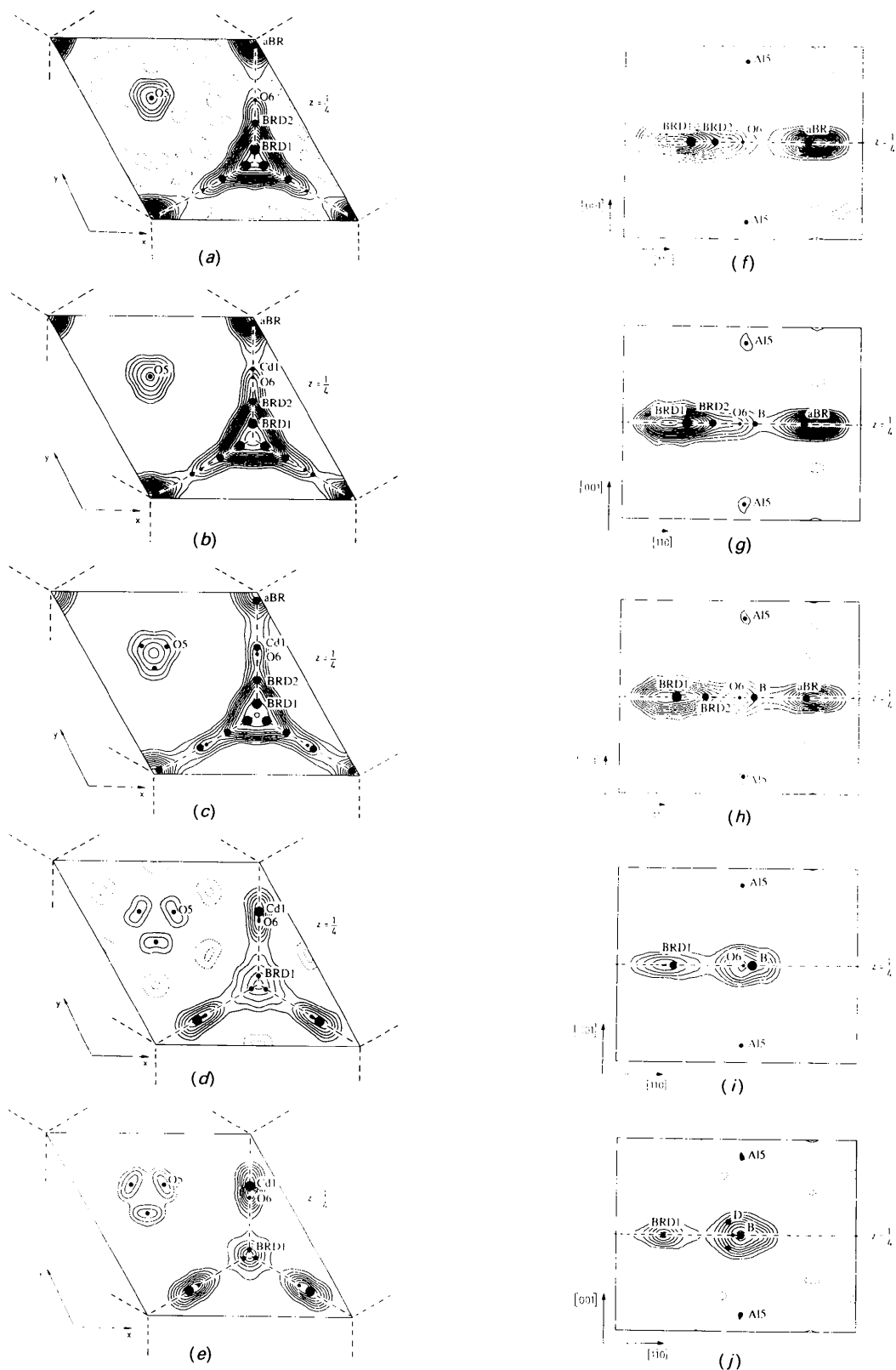
Fig. 2. F_o syntheses for $Ag_{1\cdot22-x}Cd_{y/2}Al_{11}O_{17\cdot11}$ with $y = 0\cdot00$, $0\cdot10$, $0\cdot41$, $0\cdot99$ and $1\cdot11$ (a)–(e) The conduction plane at $z = \frac{1}{4}$, (f)–(j) the $(x, -x, z)$ plane perpendicular to the conduction plane. Contour intervals are $2\cdot2$ e Å⁻³; zero contours omitted.

Table 3. *Atomic positional parameters* ($\times 10^5$) *in* $Ag_{1.22-y}Cd_{y/2}Al_{11}O_{17.11}$

Equivalent isotropic displacement parameters for the spinel block [expressed as mean-square amplitudes, $U_{eq} = \frac{1}{3}(U_{11} + U_{22} + U_{33}) \times 10^3$] and anisotropic displacement parameters ($\beta_{ij} \times 10^4$) for Ag' and Cd^{2+} ions and the O(5) atom. For each atom, the five rows refer to compositions $y = 0.00, 0.10, 0.41, 0.99$ and 1.11, respectively.

	Site	Fractional occupation	x	y	z	β_{11} or $U_{eq}(\text{Å}^2)$	β_{22}	β_{33}	β_{12}	β_{13}	β_{23}
Ag(1)	6(h)	0.168 (7)	70476 (21)	−x	¼	547 (5)	β_{11}	8.9 (1)	286 (8)	0	0
		0.168 (7)	70508 (3)			534 (2)		8.5 (1)	279 (1)		
		0.134 (7)	70254 (44)			527 (8)		8.4 (1)	317 (9)		
		0.077 (1)	70540 (80)			807 (28)		6.8 (2)	−147 (43)		
		0.037 (1)	68118 (168)			527 (11)		5.5 (2)	71 (4)		
Ag(2)	6(h)	0.105 (8)	77801 (145)	−x	¼	577 (22)	β_{11}	6.0 (2)	−353 (19)	0	0
		0.087 (2)	77801			519 (14)		6.0 (4)	−323 (1)		
		0.056 (7)	75751 (165)			297 (16)		5.4 (2)	−73 (11)		
		—	—	—	—	—	..	—	—		—
		—									
Ag(3)	6(h)	0.134 (1)	97628 (47)	−x	¼	655 (8)	β_{11}	3.8 (1)	−7.9 (15)	0	0
		0.119 (1)	97710 (21)			628 (3)		3.5 (1)	80.0 (5)		
		0.079	97604			661 (5)		3.0 (1)	84.9 (14)		
		—									—
Cd(B)	6(h)	—	—	—	—	..	..	..	.		..
		0.016	84569	−x	¼	707 (23)	β_{11}	9.0 (5)	−576 (1)	0	0
		0.069	84569			370 (5)		13.6 (3)	−63 (8)		
		0.165 (2)	85596 (41)			429 (4)		17.5 (2)	−78 (5)		
		0.154 (5)	84827 (34)			473 (4)		14.5 (2)	−101 (4)		
Cd(D)	12(k)	—	—	—				—	.	—	
		—									
		—			—	—		—	—	—	—
		0.003 (1)	82949 (38)	−x	0.2598 (1)	151 (9)	β_{11}	3.2 (4)	52 (8)	10.3 (6)	−10.3 (6)
O(2)	12(k)		50288 (6)	−x	14646 (3)	7.8					
			50287 (5)		14652 (2)	6.9					
			50269 (6)		14662 (2)	7.2					
			50276 (6)		14701 (3)	7.5					
			50265 (4)		14698 (2)	7.1					
O(3)	4(f)		⅔	⅓	5536 (5)	6.5					
					5543 (4)	5.5					
					5539 (4)	5.7					
					5587 (4)	5.7					
					5584 (3)	5.3					
O(4)	4(e)		0	0	14299 (5)	4.7					
					14301 (4)	4.8					
					14306 (4)	5.2					
					14352 (4)	5.2					
					14366 (3)	4.9					
Al(5)	12(k)	0.037	−15959 (72)	2x	17572 (33)	6.3					
			−15975 (62)		17627 (32)	5.4					
			−15880 (66)		17627 (25)	5.4					
			−15930 (68)		17657 (32)	5.8					
			−15968 (44)		17620 (22)	5.5					
O(6)	6(h)	0.037	⅚	⅙	¼	3.0					
		0.037				3.0					
		0.037				3.0					
		0.037				3.0					
		0.037				3.0					
O(5)	2(c)		⅓	⅔	¼	905 (23)	β_{11}	1.1 (3)	β_{11}.2	0	0
	6(h)		30292 (23)	−x	¼	503 (33)		0.9 (2)	159 (22)	0	0
	6(g)		29786 (5)			529 (29)		1.5 (5)	217 (20)	0	0
	6(h)		27847 (43)			456 (8)		1.5 (4)	336 (21)	0	0
	6(h)		27725 (28)			511 (4)		0.6 (2)	423 (19)	0	0
Al(1)	12(k)	0.963	−16800 (3)	2x	10650 (1)	6.3					
			−16798 (2)		10656 (1)	5.4					
			−16796 (3)		10665 (1)	5.4					
			−16798 (3)		10696 (1)	5.8					
			−16792 (2)		10709 (1)	5.5					
Al(2)	4(f)		⅓	⅔	2495 (1)	5.1					
					2490 (2)	4.1					
					2485 (2)	4.2					
					2480 (2)	4.0					
					2486 (1)	3.9					
Al(3)	4(f)		⅓	⅔	17573 (2)	7.4					
					17574 (2)	6.5					
					17577 (2)	6.7					
					17595 (2)	7.3					
					17605 (1)	6.9					
Al(4)	2(a)		0	0	0	5.6					
						4.6					
						4.5					
						4.6					
						4.4					
O(1)	12(k)		15699 (6)	2x	5020 (3)	6.4					
			15711 (5)		5018 (2)	5.4					
			15707 (5)		5017 (2)	5.4					
			15705 (5)		5033 (3)	5.5					
			15711 (3)		5036 (2)	5.3					

β-alumina (Figs. 2e and 2j). Again, Cd^{2+} ions were found at B sites and Ag$^+$ ions at BRD1 sites. A second Cd^{2+} site was refined at a D site, close to the B site but shifted out from the conduction plane in the z direction. The same type of site was also seen in fully exchanged Cd^{2+} β-alumina. The implications of this site are not clear.

The function minimized in all refinements was $\sum w(|F_o|^2 - |F_c'^2|)^2$ where $w^{-1} = \sigma^2(F_o^2) = \sigma_c^2(F_o^2) + (kF_o^2)^2$. For values of k see Table 2. Reflections with F_o^2 less than $2\sigma(F_o^2)$ were removed from the refinements. An isotropic extinction correction was applied in all refinements. The coherent scattering amplitudes and anomalous-dispersion terms used for

Table 4. *Some interatomic distances* (Å) *for* $Ag_{1\cdot22-y}Cd_{y/2}Al_{11}O_{17\cdot11}$, $y = 0\cdot00, 0\cdot10, 0\cdot41, 0\cdot99$ *and* $1\cdot11$; $P6_3/mmc$ *notation*

	$y = 0\cdot00$	$y = 0\cdot10$	$y = 0\cdot41$	$y = 0\cdot99$	$y = 1\cdot11$
Ag(1)—O(6) (×1)	1·827 (1)	1·832 (1)	1·814 (2)	1·830 (4)	1·688 (8)
Ag(1)—O(2) (×4)	2·731 (1)	2·738 (1)	2·736 (1)	2·721 (2)	2·765 (5)
Ag(1)—O(5) (×2)	3·060 (1)	2·902 (1)	2·885 (3)	2·777 (4)	2·907 (8)
Ag(2)—O(6) (×1)	2·347 (7)	2·352 (1)	2·192 (8)		
Ag(2)—O(2) (×4)	2·713 (4)	2·720 (1)	2·700 (4)		
Ag(2)—O(5) (×2)	2·847 (7)	2·636 (1)	2·660 (8)		
Ag(2)—O(6) (×1)	3·271 (7)	3·277 (1)	3·454 (8)		
Ag(3)—O(6) (×1)	1·740 (2)	1·739 (1)	1·743 (1)		
Ag(3)—O(4) (×2)	2·411 (1)	2·418 (1)	2·413 (1)		
Ag(3)—O(5) (×2)	3·120 (2)	2·835 (2)	2·778 (2)		
Cd(B)—O(5) (×2)		2·546 (1)	2·501 (3)	2·335 (3)	2·328 (2)
Cd(B)—O(6) (×1)		2·698 (1)	2·695 (1)	2·607 (2)	2·671 (2)
Cd(B)—O(4) (×2)		2·835 (1)	2·829 (1)	2·766 (1)	2·798 (1)
Cd(B)—O(2) (×4)		2·865 (1)	2·858 (1)	2·882 (1)	2·854 (1)
Al(1)—O(4) (×1)	1·821 (1)	1·825 (1)	1·822 (1)	1·821 (1)	1·820 (1)
Al(1)—O(2) (×2)	1·828 (1)	1·833 (1)	1·831 (1)	1·830 (1)	1·828 (1)
Al(1)—O(3) (×1)	1·970 (1)	1·974 (1)	1·971 (1)	1·969 (1)	1·970 (1)
Al(1)—O(1) (×2)	2·020 (1)	2·026 (1)	2·024 (1)	2·024 (1)	2·024 (1)
Al(2)—O(1) (×3)	1·799 (1)	1·802 (1)	1·801 (1)	1·800 (1)	1·799 (1)
Al(2)—O(3) (×1)	1·801 (1)	1·808 (1)	1·807 (1)	1·810 (1)	1·807 (1)
Al(3)—O(5) (×1)	1·666 (1)				
Al(3)—O(5) (×3)		1·697 (1)	1·702 (1)	1·744 (1)	1·743 (1)
Al(3)—O(2) (×3)	1·768 (1)	1·772 (1)	1·767 (1)	1·764 (1)	1·764 (1)
Al(4)—O(1) (×6)	1·892 (1)	1·897 (1)	1·894 (1)	1·894 (1)	1·894 (1)
Al(5)—O(6) (×1)	1·668 (7)	1·661 (6)	1·658 (6)	1·649 (7)	1·654 (5)
Al(5)—O(4) (×1)	1·711 (4)	1·722 (3)	1·710 (3)	1·711 (4)	1·709 (3)
Al(5)—O(2) (×2)	1·763 (4)	1·771 (3)	1·773 (2)	1·767 (3)	1·763 (2)

Al^{3+}, O^{2-}, Ag^+ and Cd^{2+} were taken from *International Tables for X-ray Crystallography* (1974, Vol. IV). All computer programs used are described by Lundgren (1982).

Positional parameters and occupations are found in Table 2 and some important distances in Table 4.*

Results and discussion

Two earlier independent room-temperature single-crystal X-ray diffraction studies of non-stoichiometric ($x = 0\cdot3$) Ag^+ β-alumina have suggested approximately equal occupation of three Ag^+ sites (Roth, 1972; Boilot, Colomban, Collongues *et al.*, 1980). Our present study corroborates these results (Figs. 2*a*, 2*f* and 3*a*); 41, 33 and 26% of the 1·22 Ag^+ ions per cell layer are localized near BRD1, aBR and BRD2 sites [Ag(1), Ag(3), Ag(2), respectively]. A more detailed description of the local ordering of Ag^+ ions is, of course, desirable but such information is not directly available from our cell-averaged diffraction picture. Our result can serve, however, as a structural basis for the main aspect of this present study; namely, to exploit the stepwise exchange of Cd^{2+} ions into the Ag^+ arrangement as a source of additional information about the Ag^+-conduction mechanism in the β-alumina host.

General structural features

The *c* axis is initially observed to increase ($y = 0\cdot10$) and only then to reverse for higher Cd^{2+} content (see Table 2). Such complex behaviour of the *c* axis is also reflected in the observed atomic arrangements within the conduction plane for different *y* values. Typically, the O(5) atom becomes more disordered (with the introduction of Cd^{2+} ions) from its 2(*c*) site ($P6_3/mmc$ notation) in Ag^+ β-alumina to 6(*h*) sites in all the Ag^+/Cd^{2+} β-alumina compositions studied. Any diffraction study of a non-stoichiometric compound such as Ag^+ β-alumina suffers from severe overlap problems, implying that bond distances and effective atomic positions are intimately related to the model used to describe the observed electron density. A more detailed analysis of the effect of ion exchange of ions within the conduction plane must therefore take account of such factors rather than speculate upon *c*-axis variations. This must be borne in mind when discussing general structural trends in these materials [see our earlier discussion in Edström *et al.* (1991)].

In the $y = 0\cdot10$ case ($\sim 8\%$ of Ag^+ replaced by Cd^{2+}), only the Ag^+ ions in the BRD2 and aBR sites are replaced (Table 2 and Figs. 2*b* and 2*g*). As more Ag^+ ions are replaced ($y = 0\cdot41$), the occupations of all three Ag^+ sites diminish at roughly equal rates, so that by the time a large percentage of the Ag^+ ions have been replaced (the $y = 0\cdot99$ and 1·11 cases) only BRD1 sites are occupied by Ag^+ ions (Figs. 2*d*, 2*e*, 2*i* and 2*j*). The Cd^{2+} ions are seen to occupy positions displaced slightly from mO [O(6)] sites (Figs. 2*e* and 2*j*), as we have seen earlier for fully exchanged Cd^{2+} β-alumina [Figs. 2*d* and 2*h* in Edström *et al.* (1991)].

The rôle of the extra oxygen, O(6)

The rôle of O(6) is of prime interest in the discussion of a possible Ag^+–Cd^{2+} ion-exchange mechanism since O(6) significantly influences the Ag^+-ion arrangement in the conduction plane. Inspecting the immediate vicinity of O(6) (Fig. 3*a*), a BRD2 site is likely to be occupied by the nearest Ag^+ ion [BRD2—O(6) 2·347 (7) Å]. The nearest aBR—O(6) and BRD1—O(6) distances are $\sim 1\cdot74$ and $\sim 1\cdot84$ Å, respectively, which are both too short to be valid Ag^+—O distances. The Ag^+—O distance in Ag_2O is $\sim 2\cdot04$ Å. The next nearest possible Ag^+ sites are also at BRD2 sites, 3·271 (7) Å from O(6).

On the assumption that Ag^+ ions are exchanged pairwise, *i.e.* that one Cd^{2+} ion exchanges two adjacent Ag^+ ions, it is reasonable to suppose that the shaded pair in Fig. 3(*a*) is the first to be exchanged for a Cd^{2+} which, in turn, takes up a stable site roughly midway between the BRD2 and the aBR site, with a Cd^{2+}—O(6) distance of 2·695 (7) Å (see

the $y = 0.10$ result). This distance can be compared with ~ 2.36 Å in CdO. It would follow then that this selective replacement will continue until all BRD2–aBR Ag^+ pairs have been removed, at around $y \simeq 0.22$. As further Ag^+ ions are replaced the occupations of all three Ag^+ sites diminish at roughly equal rates. By the time a large percentage of the Ag^+ ions have been replaced (the $y = 0.99$ and 1.11 cases), only BRD1 sites are occupied by Ag^+ ions (Figs. 2d, 2e, 2i and 2j). A reasonable interpretation here is that, between the $y = 0.41$ and 0.99 cases, there exists a composition at which all BRD2–aBR pairs have been exchanged, and Ag^+ ions only remain at BRD1 sites. A simple extrapolation of the occupations given in Table 2 gives the composition at which this occurs to be roughly $y = 0.88$, i.e. 72% of the Ag^+ ions have been replaced by Cd^{2+}. The occupation of the BRD1 sites then diminishes monotonically to zero as Cd^{2+} exchange continues. Again, a simplistic picture would maintain the existence and identity of BRD2–aBR Ag^+ pairs up to their final disappearance. It may be more realistic to imagine, however, that as increasing numbers of Cd^{2+} ions move into the system, the local repulsion effect of their $+2$ charges serves to disperse the residual Ag^+ pairs into positions of BRD1 type. The observation that all Ag^+ sites appear to deplete at approximately the same rate after this initial phase (up to $y \sim 0.22$) would suggest that subsequent Ag^+-pair exchange

occurs more or less randomly. It could well be that the Cd^{2+} ions which exchange first have a screening effect on O(6), such that other Ag^+ pairs close to O(6) are insignificantly more stable with respect to Cd^{2+} substitution than Ag^+ pairs more distant from O(6), see Fig. 3(b). The correctness of this simplistic interpretation is difficult to confirm, though we shall assume it to be the case hereafter.

Comparison with the Na^+/Cd^{2+} β-alumina system

An entirely parallel study has been made of the Na^+/Cd^{2+} β-alumina system (Edström et al., 1988, 1991) and it is therefore opportune to make some comparisons. It is immediately clear that the two cases differ qualitatively. This results directly from the ability of Ag^+ ions, in spite of their larger formal radius (1.14 compared to 0.97 Å for Na^+), to occupy the smaller aBR sites. This leads to a more extensive structural arrangement of the Na^+ pairs (Fig. 4) which then retain their identity throughout the Cd^{2+}-exchange process. With the possible exception of an Ag^+ pair close to O(6), the identity of Ag^+ pairs (perhaps even the concept of pairs) is less well defined in the Ag^+ β-alumina structure.

It is also interesting to reflect on the repercussions of this difference on the ionic conductivity for the two mixed-ion systems. In Na^+/Cd^{2+} β-alumina, the activation energy, E_a, goes through a minimum for low Cd^{2+} exchange, before rising sharply on further Cd^{2+} substitution (Sutter et al., 1983). The present structural result would suggest a less-complex behaviour for Ag^+/Cd^{2+} β-alumina, as a result of the less extended nature of the Ag^+ ordering around O(6). No reliable conductivity data are yet available for this system, however.

To summarize, it has been seen that differences in the nature of the local interactions of Na^+ and Ag^+ ions with their chemical environments lead to qualitative differences in ionic arrangement and ion-exchange mechanism. Implicit in this result is that ion-transport mechanisms in the Na^+ and Ag^+ β-alumina systems will also be qualitatively different in the two cases. A general observation is that conventional diffraction techniques have been successful here in exposing evidence for these differences.
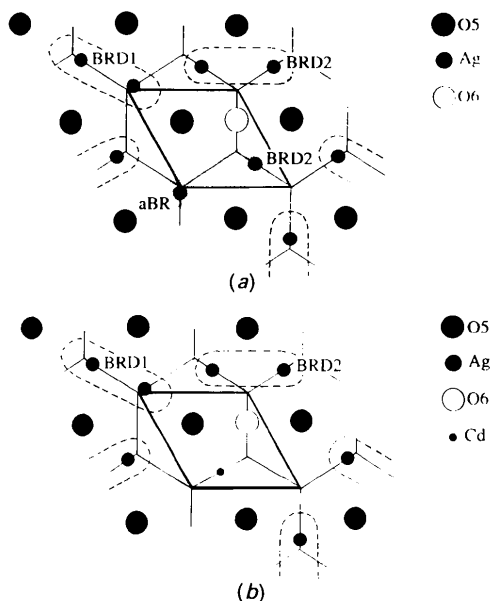
Fig. 3. Local structurization for Ag^+ ions around O(6) in (a) Ag^+ β-alumina; the pair of Ag^+ ions first replaced for Cd^{2+} is shaded in. The situation shown in (b) corresponds to $y = 0.22$, in which Cd^{2+} ions have replaced the first Ag^+-ion pair, and the remaining arbitrarily defined Ag^+ pairs are indicated with dashed lines.
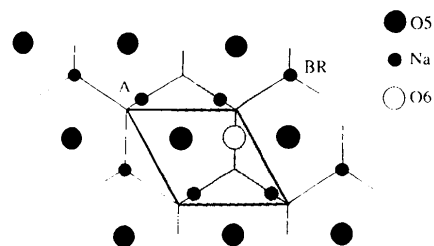
Fig. 4. The sphere of greatest influence on the Na^+ ions around O(6) in Na^+ β-alumina.

References

BLESSING, R. H., COPPENS, P. & BECKER, P. (1974). *J. Appl. Cryst.* **7**, 488–492.

BOILOT, J. P., COLOMBAN, P., COLLIN, G. & COMÈS, R. (1980). *J. Phys. Chem. Solids*, **41**, 47–54.

BOILOT, J. P., COLOMBAN, P., COLLONGUES, R., COLLIN, G. & COMÈS, R. (1980). *J. Phys. Chem. Solids*, **41**, 253–258.

BRUCE, J. A., HOWIE, R. A. & INGRAM, M. D. (1986). *Solid State Ionics*, **18–19**, 1129–1133.

CATTI, M., CAZZANELLI, E., IVALDI, G. & MARIOTTO, G. (1987). *Phys. Rev. B*, **36**, 9451–9460.

EDSTRÖM, K., THOMAS, J. O. & FARRINGTON, G. C. (1988). *Solid State Ionics*, **28–30**, 363–368.

EDSTRÖM, K., THOMAS, J. O. & FARRINGTON, G. C. (1991). *Acta Cryst.* **B47**, 635–643.

LEHMANN, M. S. & LARSEN, F. K. (1974). *Acta Cryst.* **A30**, 580–584.

LUNDGREN, J.-O. (1982). *Crystallographic Computer Programs.* Report UUIC-B13-04-05. Institute of Chemistry, Univ. of Uppsala, Sweden.

MCCANDLISH, L. E., STOUT, G. H. & ANDREWS, L. C. (1975). *Acta Cryst.* **A31**, 245–249.

REIDINGER, F. (1979). PhD Thesis, State Univ. of New York, Albany, USA.

ROTH, W. L. (1972). *J. Solid State Chem.* **4**, 60–75.

ROTH, W. L., REIDINGER, F. & LaPLACA, S. (1976). *Superionic Conductors*, edited by G. D. MAHAN & W. L. ROTH, pp. 223–241. New York: Plenum Press.

SUTTER, P. H., CRATTY, L., SALTZBERG, M. & FARRINGTON, G. C. (1983). *Solid State Ionics*, **9–10**, 295–298.

TOFIELD, B. C. & FARRINGTON, G. C. (1979). *Nature (London)*, **278**, 438–439.

YAO, Y. F. & KUMMER, J. T. (1967). *J. Inorg. Nucl. Chem.* **29**, 2453–2474.

Charge Densities in CoS₂ and NiS₂ (Pyrite Structure)

BY ELLEN NOWACK

Institut für Kristallographie, RWTH Aachen, Templergraben 55, D-5100 Aachen, Germany

DIETER SCHWARZENBACH

Institut de Cristallographie, Université de Lausanne, Bâtiment des Sciences Physiques, Dorigny, CH-1015 Lausanne, Switzerland

AND THEO HAHN

Institut für Kristallographie, RWTH Aachen, Templergraben 55, D-5100 Aachen, Germany

Dedicated to Professor Karl Fischer on the occasion of his 65th birthday

Abstract

The electron-density distributions in the pyrite-type structures of CoS_2 and NiS_2 have been determined from high-resolution single-crystal diffraction data [Ag $K\alpha$ radiation; resolution and temperature $(\sin\theta/\lambda)_{max} = 1\cdot49$ Å^{-1} at 295 K for CoS_2, $1\cdot63$ Å^{-1} at 135 K for NiS_2]. The charge densities were refined using a multipolar deformation model [$R(|F|) = 0\cdot0119$ and $0\cdot0136$, respectively]. The X-ray diffraction data of FeS_2 [Stevens, DeLucia & Coppens (1980). *Inorg. Chem.* **19**, 813–820; Ag $K\alpha$ radiation, $(\sin\theta/\lambda)_{max} = 1\cdot46$ Å^{-1}, room temperature] were refined using the same deformation model and program in order to facilitate comparison of the results [$R(|F|) = 0\cdot0176$]. The main features of the result- ing deformation maps agree well for all three structures. They consist of important maxima in the immediate vicinity of the metal atoms pointing towards the faces of the coordination octahedron. The heavier the metal atom, the smaller is the distance of the maxima from the atomic centre. These features are interpreted by a preferential occupation of the metal d orbitals which correspond to the cubic t_{2g} orbitals. An analysis of the d-orbital populations indicates that the symmetry of the electron distribution around the metal atom is in all cases very close to cubic, the site symmetry being $\bar{3}$; the t_{2g} orbitals appear to be fully occupied by six electrons while the occupation of the e_g orbitals increases in the series Fe, Co, Ni and indicates covalent overlap with the S ligands.